Colloids and Surfaces A 532 (2017) 397–404

Contents lists available at ScienceDirect

Colloids and Surfaces A

journal homepage: www.elsevier.com/locate/colsurfa

Aggregation of colloidal spheres mediated by Janus dimers: A Monte Carlo study

Gianmarco Munaò*, Dino Costa, Santi Prestipino, Carlo Caccamo

Dipartimento di Scienze Matematiche e Informatiche, Scienze Fisiche e Scienze della Terra, Università degli Studi di Messina, Viale F. Stagno d'Alcontres 31, 98166 Messina, Italy

GRAPHICAL ABSTRACT

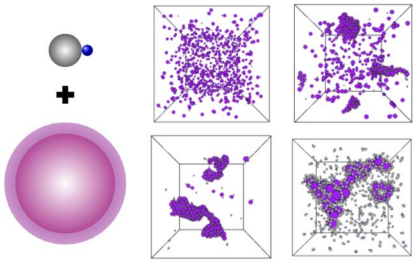

ARTICLE INFO

Keywords:
Colloids
Self-assembly
Monte Carlo

ABSTRACT

We investigate by Monte Carlo simulation the structure and self-assembly of a mixture formed by asymmetric dimers and larger spherical particles. In our model, dimers and spheres interact through a monomer-specific short-range attraction, in addition to hard-core repulsion. The interaction parameters are chosen so as to mimic features of real colloidal mixtures. We find that the dilute mixture at low temperature is characterized by the onset of aggregates of spheres held together by dimers. In particular, when the sphere concentration is sufficiently high, the system stays homogeneous; at intermediate concentrations, very small clusters of spheres coexist with a few lamellar aggregates; finally, for even lower concentrations a single droplet eventually forms. Upon increasing the density, a sponge-like structure emerges for not too high concentrations. If the attraction between dimers and spheres is switched off, leaving only depletion forces to act, neither phase separation nor demixing are found.

1. Introduction

Colloidal dispersions are an important class of materials, which can be both inorganic (like paints or glues) and organic (milk, blood, etc.). Their phase behaviour is very rich, due to the endless possibilities to combine the size, shape, and concentration of the constituents, which makes colloids among the most investigated substances of soft matter [1–3]. In view of the ability of solute particles, either natural or artificially designed, to spontaneously organize in complex structures, the study of colloids has gained increasing relevance in the last years for the fabrication of complex architectures on the nanoscale [4–8]. A clear control of self-assembled structures is the key to optimize the performance and response of colloids in many industrial applications [9,10].

Stable mixtures of different solute species are ubiquitous, and even more versatile then one-component colloids. Generally, the components of a colloidal mixture do not separate in equilibrium, at least provided that the temperature is high enough [1]. Experimentally this goal is obtained by adding a surfactant coating to the colloidal particles, in order to avoid flocculation and keep them dispersed [11]. When cooled to a sufficient degree, colloidal mixtures may phase separate/demix

* Corresponding author.
E-mail address: gmunao@unime.it (G. Munaò).

http://dx.doi.org/10.1016/j.colsurfa.2017.04.054
Received 27 February 2017; Received in revised form 21 April 2017; Accepted 23 April 2017
Available online 19 May 2017
0927-7757/

[12] or form aggregates (micelles, clusters, lamellae, etc.) [13,14], as a result of the attractive forces between the particles. To a large extent, colloidal solutions can be modelled as systems of macroparticles with effective interactions implicitly accounting also for the solvent; the Asakura–Oosawa and the DLVO theories [15] are well-known examples of such an approach that, despite its simplicity, allows to make sense of complex phase behaviours, including vitrification and gelation [16–18]. Binary mixtures of repulsive and attractive particles are extensively investigated (see e.g. Refs. [19,20]), with the observation of a rich variety of phase behaviours. Even mixtures of repulsive particles of largely different sizes may separate under certain conditions, due to depletion effects [21–25]; such entropy-driven interactions arise from a large difference in size between the species in solution, resulting in a net attraction between the bigger particles. For instance, it has been shown that largely asymmetric hard-sphere mixtures may experience a demixing transition [26,27].

We here study a model mixture composed by asymmetric dimers and spheres; a short-range attraction is only placed between a sphere and the smaller monomer in a dimer. Spheres are three times bigger than dimers and a narrow (square-well) attraction is adopted, so as to reproduce a range of sizes and interactions arising in real mixtures of colloidal particles. Within our model, the dimer behaves as made of a solvophobic particle, namely the small monomer, and an inert large monomer, whence the designation of Janus (i.e. amphiphilic) dimers. Viable routes for a practical realization of our model mixture have been presented in the recent literature: for example, in Refs. [28,29] the authors have demonstrated that Janus dimers with single seeds in the sub-micrometre domain (precisely, in the range 50–200 nm) can be successfully synthesized. Moreover, the possibility to graft DNA strands on the colloidal surface allows to customize the effective interaction: it has been shown [30,31] that two types of DNA strands, differing in their sticky ends, can lead either to an attractive interaction or to a simple steric repulsion. Very recently, a colloidal mixture closely resembling our model system has been prepared and experimentally studied in Ref. [32].

The main focus of the present study is on aggregation of spheres mediated by Janus dimers. We employ the Monte Carlo simulation to provide a full description of the fluid behaviour as a function of density, concentration, and temperature. The properties of our mixture are also contrasted with that of the same system in the absence of attraction, so as to ascertain the different abilities of depletion forces and explicit attraction to promote non-trivial self-assembled structures. This study follows two recent investigations we have carried out on the same model mixture [33,34]. In Ref. [33] spheres were taken to be as large as the larger of the two monomers and we observed a variety of aggregates as a function of the relative concentration of the two species. In Ref. [34], the size ratios among the various species were equal to those employed here, but the dimer-sphere attraction had a longer range; in that case we found that, for vanishing concentration, spheres get coated with dimers, thus giving rise to capsules; conversely, for higher sphere concentrations a separation is observed between a sphere-rich and a sphere-poor phase.

This paper is organized as follows. In Section 2 we describe our model and the simulation technique. Results are presented and discussed in Section 3. Concluding remarks and perspectives finally follow in Section 4.

2. Models and methods

A picture of the particles in our mixture is drawn in Fig. 1: the dimer is a pair of tangent hard-sphere monomers (labelled 1 and 2) with core diameters $\sigma_1 = \sigma_2/3$, while spheres (species 3) have a hard core of diameter $\sigma_3 = 3\sigma_2$. All interactions are purely excluded-volume, with additive diameters $\sigma_{ij} = (\sigma_i + \sigma_j)/2$, except for an additional square-well attraction between the smaller monomer and a sphere, at mutual distance r_{13}:

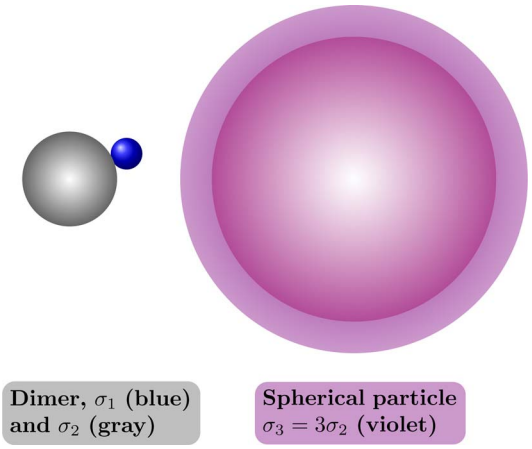

Fig. 1. The model mixture studied in this work: Janus dimer with size ratio $\sigma_1/\sigma_2 = 1/3$ (left) and spherical particle of diameter $\sigma_3 = 3\sigma_2$ (right). The shaded area around the sphere indicates the bonding region, extending up to $r_{13} = \sigma_{13} + \sigma_1$.

$$\phi_{sw}(r_{13}) = \begin{cases} \infty & \text{if } r_{13} < \sigma_{13} \\ -\varepsilon & \text{if } \sigma_{13} \le r_{13} < \sigma_{13} + \sigma_1 \\ 0 & \text{otherwise.} \end{cases} \quad (1)$$

The attraction range has been chosen so as to be small in comparison with the diameter of the spherical particle, as is typical of colloidal systems, and equal to the size of the small monomer. Moreover, no mutual attraction is placed between two dimers or between two spheres, in the assumption that such interactions (which are usually also present in real colloids) are much weaker than ϕ_{sw}.

We observe that the condition $\sigma_1/\sigma_2 = 1/3$ favours the formation of aggregates of spherical shape in a fluid of amphiphilic dimers, in agreement with the empirical rule [35]:

$$\frac{V}{A \times L} \le \frac{1}{3}, \quad (2)$$

where V is the dimer volume, A its surface area, and L its length. Finally, with the above choice of particle diameters we have also the possibility to investigate the relative efficacy of ϕ_{sw} and depletion attraction to promote the onset of aggregates in the mixture upon cooling.

We have studied thermodynamic, structural, and self-assembly properties of a binary mixture composed of a total of $N = 1000$ particles, by means of standard Monte Carlo (MC) simulations in the canonical ensemble, with periodic conditions at the box boundaries (for more details, see Ref. [33]). We denote with N_d and $N_s \equiv N - N_d$ the numbers of dimers and spheres, respectively. The concentration of spheres is then given by $\chi \equiv N_s/N$, with packing fraction $\eta = (\pi/6)\rho\chi\sigma_3^3$, ρ being the number density of the mixture. In the following, σ_3 and ε are taken as units of length and energy, respectively, with the reduced temperature then defined as $T^* = k_B T/\varepsilon$, k_B being Boltzmann's constant.

In the aim to characterize the mixture over a wide range of thermodynamic conditions and different compositions, we have studied four different samples, starting from pure hard spheres (i.e. $\chi = 100\%$), at increasing packing fractions from very dilute to relatively dense conditions ($\eta = 0.014$, 0.028, 0.14, and 0.28). Next, we have altered the balance between N_s and N_d, so as to first bring the concentration of spheres down to 80% and then halving this value four times (i.e. reducing χ successively to 40%, 20%, 10% and 5%). With the obvious exception of the athermal hard sphere fluid, all remaining twenty samples have been prepared at $T^* = 0.30$ and then cooled down to $T^* = 0.20$ and $T^* = 0.15$. For $T^* = 0.30$ we have first performed 5×10^5 MC steps per particle (cycles) in order to equilibrate the system, then computing statistical averages over the next million cycles. For the lowest temperature investigated ($T^* = 0.15$), we have carried out one to four hundred million cycles, depending on the concentration,

in order to ensure a proper equilibration and an accurate determination of statistical properties.

In order to characterize the aggregation properties of the spheres, as promoted by the gradual addition of dimers to the mixture, we have carried out a microscopic cluster analysis on a few state points. To this aim, two spheres are considered as bound if their distance reaches at most the position of the first minimum of the radial distribution function, $g_{33}(r)$. We have identified all particle aggregates through the Hoshen–Kopelman algorithm [36], readily generalized to the continuum. For the analysis, we have considered a thousand of evenly-spaced configurations out of a slice of ten million MC cycles. We have thus computed several statistical properties of the aggregates, namely the fraction of isolated particles, the number of clusters, and the size of the largest cluster in each configuration. The cluster-size distribution (CSD), $N(s)$, has been normalized according to the expression:

$$n(s) = \frac{s\,N(s)}{N_s} \tag{3}$$

where s is the cluster size [37–40]. The function $n(s)$ represents the average fraction of particles contained in all clusters of size s, as opposed to the average number $N(s)$ of s-clusters in one configuration. Finally, in reporting pictures of microscopic configurations, and in order to avoid the possible split of a cluster across the box boundary, we have first identified the cluster centre of mass using the method devised by Bai and Breen [41] (which maps cartesian coordinates to a torus, see also the Wiki page [42]). Then, for each particle belonging to a given cluster, we have plotted the replica closest to the centre of mass.

3. Results

We first discuss the properties of the mixture with a packing fraction of spheres $\eta = 0.014$, i.e. in the most dilute conditions for this species among those investigated in this work. In Fig. 2 we report the structural properties at different temperatures and sphere concentrations, namely $\chi = 100\%$ (pure fluid of spheres), 80%, 40%, 20%, 10% and 5%. For $T^* = 0.30$ (a), the sphere-sphere structure factor $S_{33}(k)$ is characterized by a modest main diffraction peak for $k\sigma_3 \approx 2\pi$, while being almost structureless beyond this k, with a small $k \to 0$ limit indicating a low compressibility in all samples, independently of the relative concentration of the two species. All evidence shows that $T^* = 0.30$ is a temperature high enough that the system is homogeneous for all concentrations. Hints of a non-trivial role of the concentration are instead observed for $T^* = 0.20$ (b); there, we see the rise of $S_{33}(k)$ in the zero-k region for $\chi \leq 20\%$, which marks the onset of large density fluctuations in the fluid. A clearly inhomogeneous structure eventually develops for $T^* = 0.15$ (c); compared to $T^* = 0.20$, also the fluid with $\chi = 40\%$ is now affected by large density fluctuations, whereas for $\chi = 80\%$ the mixture apparently remains homogeneous. This low-T picture is confirmed by the local ordering of the spheres, as clarified by the profile of $g_{33}(r)$ (d). For $\chi = 80\%$, ideal-gas behaviour sets in immediately after a thin first coordination shell. A sharp enhancement of local spatial correlations is instead observed for $\chi \leq 40\%$, which again points to the existence of large density fluctuations in the system, possibly implying a phase separation. Another indication that we are close to a phase-separated state at low χ is the slow large-distance decay of $g_{33}(r)$.

Further insight into the phase portrait of the mixture can be gained by visual inspection of the microscopic configurations: in Fig. 3 we report typical configurations of the equilibrated system for $T^* = 0.15$, at all sphere concentrations. In the absence of dimers, the fluid of hard spheres is obviously homogeneous (a), and this condition is barely affected by the addition of a few dimers ($\chi = 80\%$, b). On the opposite side, i.e. for $\chi \leq 20\%$ (bottom panels), the mixture clearly separates into a colloid-rich and a colloid-poor phase. Apparently, phase separation is best resolved for $\chi = 20\%$, where almost all particles in the mixture belong to a single rather compact aggregate. For lower concentrations, the system encounters more difficulties to exploit a full separation of phases. Different factors contribute to this outcome: a first reason is that a too large number of dispersed dimers eventually leads to the formation of a coating shell around each aggregate of spheres; once such “capsules” are formed, the outer layer of type-2 particles hinders the possibility for distinct aggregates to coalesce together. A second, more technical reason is related to the increasing difficulty encountered by the sample, as the number of dimers increases, to relax to equilibrium after a reasonably long, but finite simulation run; indeed, spheres tend to be trapped in the sea of small particles, and hence their mobility and related tendency to form aggregates are greatly frustrated. Instead, for $\chi = 20\%$ spheres are still relatively mobile, and their number optimally match that of dimers, hence spheres are able to

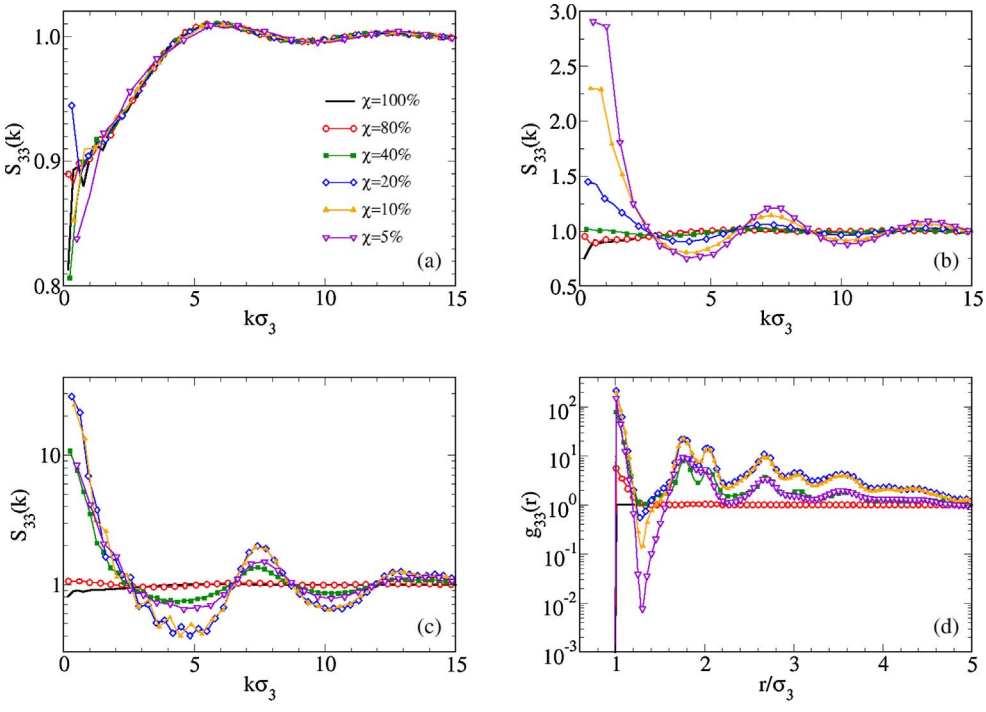

Fig. 2. Structural correlations for a sphere packing fraction of $\eta = 0.014$ and all sphere concentrations (in the legend): $S_{33}(k)$ for $T^* = 0.30$ (a), 0.20 (b), and 0.15 (c); $g_{33}(r)$ for $T^* = 0.15$ (d).

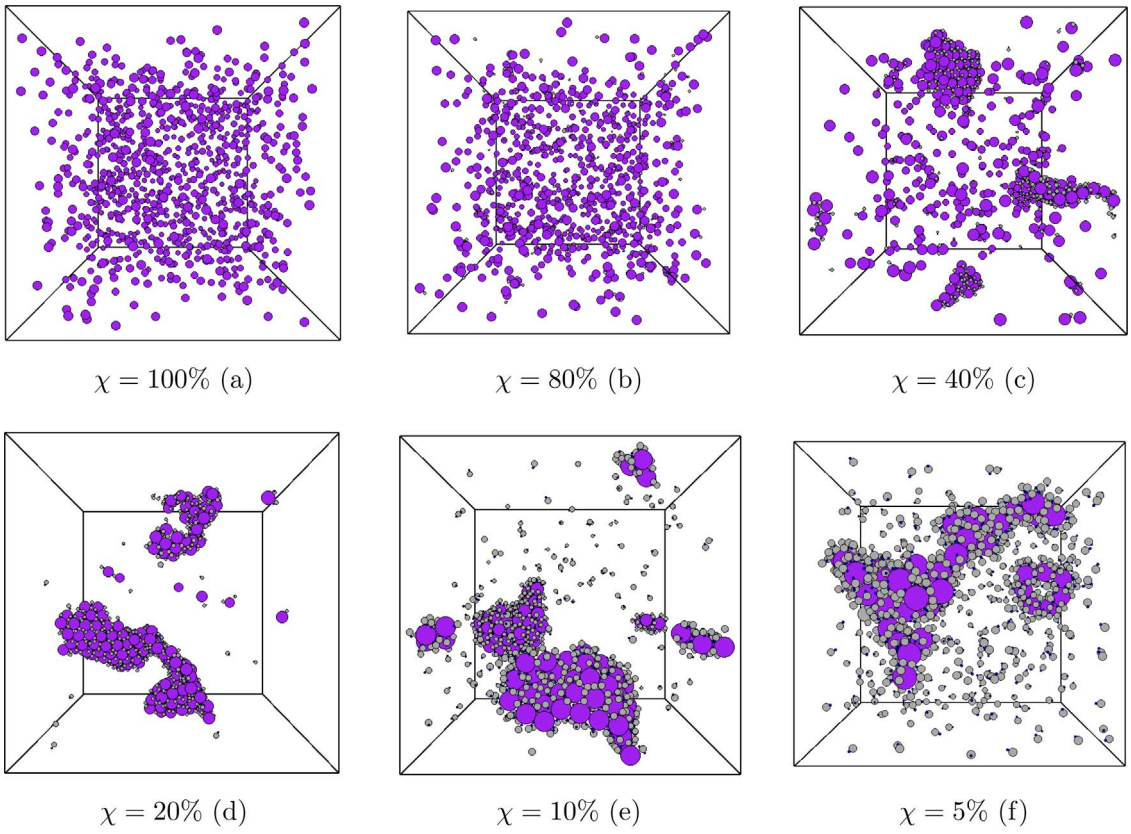

Fig. 3. Snapshots of typical microscopic configurations for a sphere packing fraction of $\eta = 0.014$ and all sphere concentrations ($T^* = 0.15$).

attain a final state corresponding to a unique droplet in coexistence with a few isolated particles.

A peculiar scenario emerges at intermediate concentrations: as is clear from Fig. 3c, for $\chi = 40\%$ the mixture is neither completely homogeneous nor well phase-separated; rather, a few lamellar aggregates are seen to coexist with small clusters and isolated spheres. This point can be better appreciated from Fig. 4, where a different rendering of the same configuration in Fig. 3c is reported; here, only sphere aggregates are drawn and discriminated by different colours according to their size. We have carried out the cluster analysis of this single microscopic configuration according to the procedure described at the end of the previous section, assuming a bond distance between two spheres equal to $1.33\sigma_3$ (corresponding to the position of the first minimum in $g_{33}(r)$, see the curve with squares in Fig. 2d). As we see in Fig. 4, the largest aggregates in the sample (coloured in green and red) are compact, roughly planar objects; therein, spheres are arranged in a curved sheet with triangular-crystal order, which in at least one case (red aggregate) is probably the outcome of a past collision event between two smaller lamellae with tilted orientations. Also in our previous study [33], relative to $\sigma_3 = \sigma_2$, we found lamellar aggregates showing up at intermediate concentrations, but in that case the ordering of spheres was different (a square bilayer rather than a triangular lattice). We surmise that, in the present case, a larger availability of "gluing" dimers within each lamella provides a nearly isotropic short-range attraction between two neighbouring spheres, which in turn promotes close-packed arrangements. Indeed, a certain degree of crystallinity is also apparent in the aggregates seen in Fig. 3d and e, which neatly distinguishes the present condensates from the much more disordered aggregates found for a longer-ranged 1–3 attraction [34].

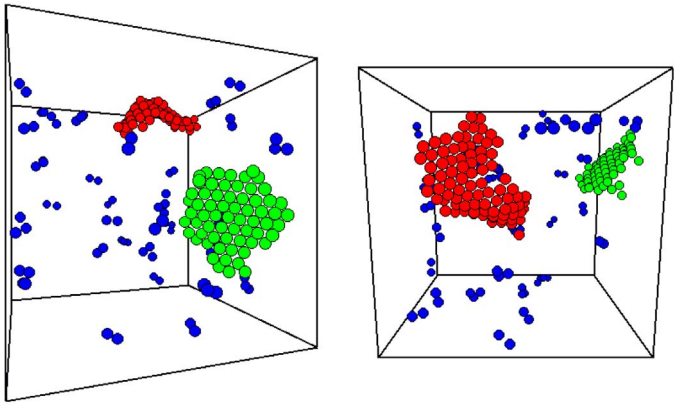

Fig. 4. Typical microscopic appearance of the system for $\eta = 0.014$ and $\chi = 40\%$ of spheres (for $T^* = 0.15$). For the sake of clarity, dimers and isolated spheres are not shown. In the two panels, the same configuration is shown from different viewpoints. The two lamellae are coloured in red and green; remaining small clusters in blue. (For interpretation of the references to colour in this figure legend, the reader is referred to the web version of this article.)

When extending the cluster analysis to a whole slice of the MC trajectory for $\chi = 40\%$, roughly one half of the spheres are found to be isolated, another sixth participates in clusters of two-four spheres, while the remaining spheres are bound together to form the lamellae. The full CSD, Eq. (3), is reported in Fig. 5 (squares). While at earlier times the shape of the distribution was as expected for a cluster fluid [39,40], with a characteristic non-monotonous trend and a local peak at the preferred cluster size, as simulation progresses two well-definite peaks eventually develop in correspondence with the size of the lamellae seen in Fig. 4. In Fig. 5 the asymptotic profile of the CSD for $\chi = 40\%$ is contrasted with that relative to a homogeneous state ($\chi = 80\%$, circles) and with that for a fully phase-separated state ($\chi = 20\%$, diamonds); for the homogeneous fluid, the CSD is characterized by a sharp decrease of the probability associated with the formation of dimers, trimers, and so on, and already vanishes for $s \approx 10$. On the opposite side, in the phase-separated state small aggregates are practically absent, and the

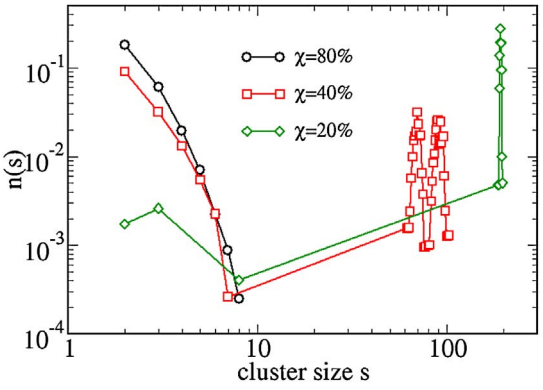

Fig. 5. Cluster size distribution, Eq. (3), for $\eta = 0.014$ and a number of sphere concentrations, in the legend ($T^* = 0.15$). Notice that s is just the number of spheres in the cluster (the cluster contains also dimers).

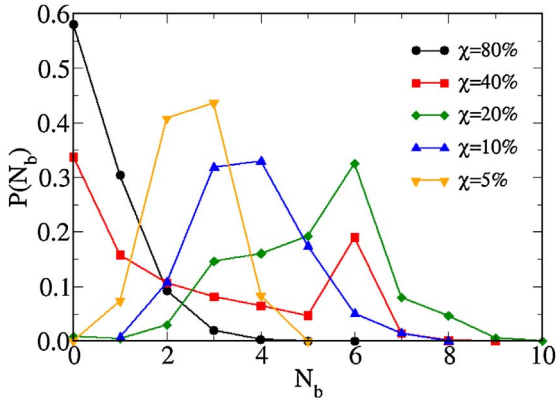

Fig. 7. Probability distribution of bonds among spheres for a sphere packing fraction of $\eta = 0.028$ and all sphere concentrations, in the legend ($T^* = 0.15$).

distribution is characterized by a single narrow peak, corresponding to the aggregate seen in Fig. 3d.

The question naturally arises as to whether what discussed so far truly corresponds to the equilibrium conformation of the system. To this aim, we have resorted to the complementary analysis of the potential energy, reported in Fig. 6. In (a), the average energy per particle, $\langle E/N \rangle$, is plotted as a function of concentration; we see that this quantity first decreases as χ is lowered, until a minimum is attained for $\chi = 20\%$, followed by a recovery for even lower concentrations. Hence, the energy content of the mixture is maximized (in absolute value) for an optimal degree of mixing of dimers and spheres, corresponding to $\chi = 20\%$; as remarked before, this is the best condition for a well-resolved phase separation to occur. Looking at the energy evolution (Fig. 6b), we see that the current E/N is apparently well relaxed for both high and low concentrations, while a very slow downward drift still persists for $\chi = 10\%$, 20%, and 40% (see panel c). This suggests that minor conformational rearrangements of large aggregates are still possible at such concentrations, whereas the lowest-χ samples are probably unable to evolve towards a "cleaner" phase-separated state. This may also explain why the energy is higher at lower concentrations, despite the fact that a larger availability of dimers would in principle favour the creation of contacts.

We now consider the effects of progressively increasing the packing fraction of spheres. It first turns out that the picture emerging for $\eta = 0.014$ is barely modified when moving to $\eta = 0.028$. In Fig. 7 we report the distribution $P(N_b)$ of the number of spheres bound to a central sphere, for $T^* = 0.15$ and all concentrations. As in the previous $\eta = 0.014$ case, for $\chi = 80\%$ the system is practically homogeneous: most spheres are isolated, and $P(N_b)$ falls rapidly to zero as N_b increases. For $\chi = 40\%$, $P(N_b)$ develops a peak at $N_b = 6$, indicating planar triangular order. For $\chi = 20\%$, more than 30% of the spheres are still bound to other six spheres whereas, for lower concentrations, the maximum of $P(N_b)$ moves to a smaller number of neighbours: indeed, similarly as for $\eta = 0.014$, for a concentration of 10% or lower, the hindrance effect caused by the many dispersed dimers prevent a large number of spheres from gathering together, again leading to an incomplete phase separation. Snapshots of indicative microscopic configurations are reported in Fig. 8: compared to the corresponding pictures for $\eta = 0.014$ (Fig. 3), the onset of aggregates again takes place near $\chi = 40\%$ (c), with a typical size now slightly larger. We surmise that the branched structure of the condensate for $\chi = 20\%$ (d) eventually evolves to a more compact "droplet" in a substantially longer simulation run. The discussion about the onset and nature of the phase separation at lower concentrations (e and f) goes along the same lines as for $\eta = 0.014$.

Significant differences instead arise when increasing the density of spheres by one order of magnitude ($\eta = 0.14$). In short, the snapshots of microscopic configurations in Fig. 9 show that local inhomogeneities first take place for $\chi = 40\%$ (c), where a sponge-like, percolating network of spheres is seen. Such inhomogeneities can be viewed as voids in a much denser environment (c-f). This picture, where vapour "bubbles" are immersed in a denser environment, is perfectly specular to the observation of droplets in an almost structureless vapour for $\eta = 0.014$. It is worth comparing these results with those obtained in Ref. [34] for the same mixture, but with a longer-ranged attraction between dimers and spheres ($2.5\sigma_1$ instead of σ_1): in that case, a separation between a sphere-rich and a sphere-poor phase was evident for both $\eta = 0.14$, $\chi = 20\%$ and $\eta = 0.07$, $\chi = 10\%$; moreover, a slab-like structure was observed for $\chi = 20\%$ whereas a cylindrical arrangement was found for $\chi = 10\%$. We have no evidence of similar arrangements here, even though phase separation also occurs in the present model. We are then led to the conclusion that the development of more symmetrical droplets sensitively depends on the range of the dimer-sphere attraction.

As a last issue, we study the effect of switching off the attraction ϕ_{sw} (which is equivalent to taking the infinite-temperature limit of our system), so as to determine to what extent the phase portrait of the

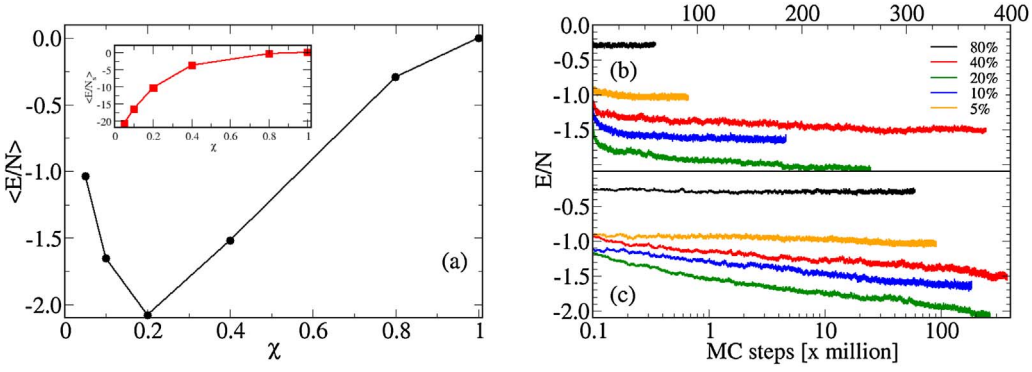

Fig. 6. Potential energy for $\eta = 0.014$ and $T^* = 0.15$: (a): average value per particle (main panel) and per sphere (inset) vs sphere concentration. Current value per particle vs MC steps in normal (b) and semilogarithmic (c) scales. (For interpretation of the references to color in this figure legend, the reader is referred to the web version of this article.)

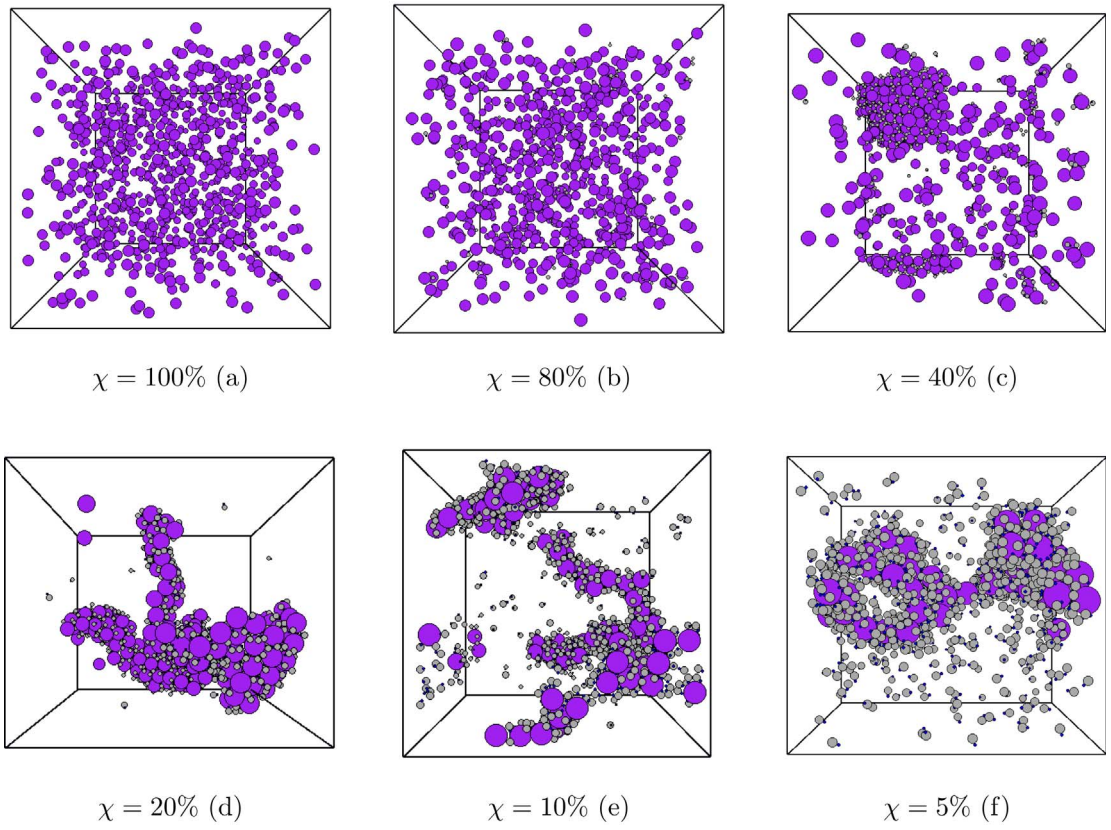

Fig. 8. Snapshots of typical microscopic configurations for a sphere packing fraction of $\eta = 0.028$ and all sphere concentrations ($T^* = 0.15$).

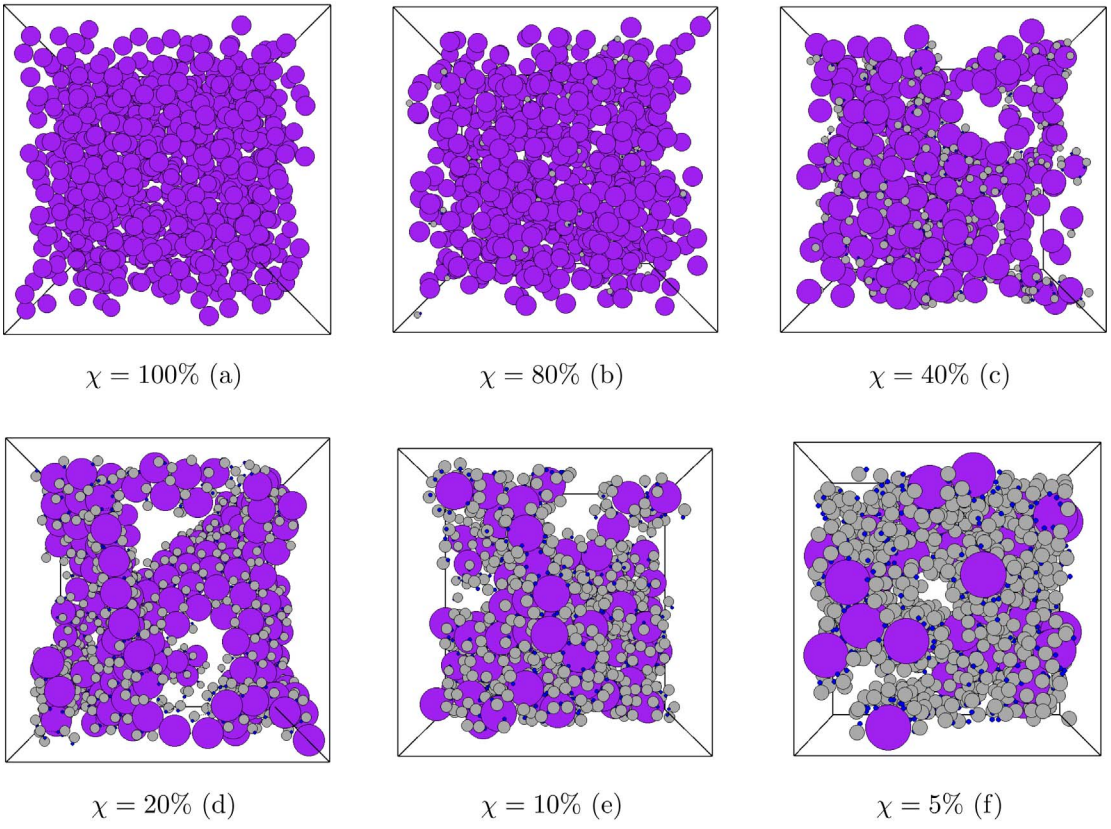

Fig. 9. Snapshots of typical microscopic configurations for a sphere packing fraction of $\eta = 0.14$ and all sphere concentrations ($T^* = 0.15$).

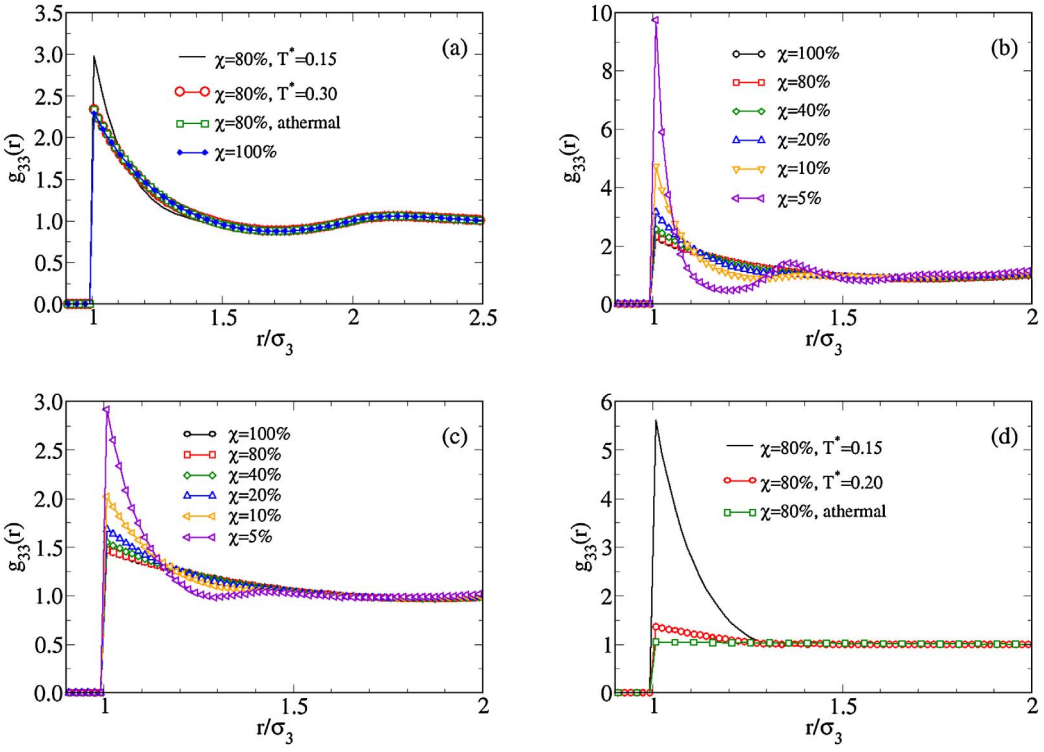

Fig. 10. Comparison between $g_{33}(r)$ with and without the ϕ_{sw} attraction, for sphere packing fractions of $\eta = 0.28$ (a, b), $\eta = 0.14$ (c), and $\eta = 0.014$ (d), and different sphere concentrations (in the legends). In (a) and (d) data for the system without attraction are marked as "athermal"; in (b) and (c), all curves exclusively refer to the athermal mixture.

mixture depends on the interplay between explicit attraction and depletion forces. Moreover, we shall see below that the attraction also plays a role for large χ values, at least for the low-density mixtures. The results of our analysis are reported in Fig. 10, where we show $g_{33}(r)$ for distinct types of interactions and several densities and concentrations. We first discuss the case of a high density of spheres, where depletion effects are expected to be strongest. In (a), which refers to $\eta = 0.28$, the structure of the fluid is mainly determined by the high packing of spheres: adding a moderate amount of dimers, switching on/off the attraction, and playing with temperature all have little effect on the behaviour of the pure hard-sphere fluid. In (b), which refers to $\eta = 0.28$ and all concentrations, the inclusion of a progressively large number of dimers strongly changes the local structure of the athermal mixture, with a better resolved first coordination shell and the development of secondary oscillations at the lowest concentrations. These structural modifications do not change the overall homogeneous fluid condition and hence they turn out to be rather irrelevant as compared to the effects of inter-species attraction. Similar considerations apply for the case $\eta = 0.14$ (c), with the only difference that the effects related to a decrease of concentration appear now smoother with respect to $\eta = 0.28$. Finally, we expect that the attraction plays a major role at low density, where depletion interactions are instead ineffective. As seen in (d), this is indeed the case: for $\eta = 0.014$ and $\chi = 80\%$, the system tends to stay overall homogeneous, regardless of whether the attraction is present or not; however, in the former case the strength and extension of first-neighbour correlations are larger. This effect is particularly evident as the temperature drops from 0.20 to 0.15. In summary, even though simple hard-core exclusion is able to promote an effective attraction between spheres (especially relevant at high density), such mutual forces, if only for the specific modelization and thermodynamic conditions investigated in this work, are definitely too weak to induce phase separation or cluster formation.

4. Conclusions

We have studied, by extensive Monte Carlo simulations, the phase behaviour of a model colloidal mixture of Janus dimers and larger hard spheres. Dimers are composed by a pair of tangent monomers with size ratio $\sigma_1 = \sigma_2/3$, while spherical particles are quite bigger ($\sigma_3 = 3\sigma_2$). In addition to excluded-volume interactions, small monomers and spheres also interact via a short-range attraction, of range σ_1.

Mixtures are initially prepared with spheres only, at different packing fractions η ranging from dilute to dense conditions; then, a progressively large number of dimers is added, so as to decrease the concentration of spheres from the pure condition ($\chi = 100\%$) down to $\chi = 5\%$. In dilute conditions ($\eta = 0.014$), and when spheres are largely predominant ($\chi \geq 80\%$), the system is always homogeneous. Upon decreasing the concentration of spheres, inhomogeneities gradually build up, until definitely dominating for low temperatures; in particular, for $\chi = 40\%$ spheres are organized in a few lamellar aggregates coexisting with a fluid of small clusters; if the concentration is further reduced ($\chi = 20\%$), a separation is observed into a colloid-rich and a colloid-poor phase. For $\chi < 20\%$, phase separation is less resolved, essentially because of the hindrance effects exerted by dimers on the growth of sphere aggregates. This phase scenario remains unchanged when doubling the original packing fraction. For $\eta = 0.14$ and above, the cluster fluid disappears; coherently with the high density of the samples, the (incomplete) phase separation manifests itself as a sponge-like structure (i.e. vapour bubbles in a denser environment), rather than as droplets in a vapour phase, as observed at dilute conditions.

In order to elucidate whether excluded-volume effects alone are capable to give the same phenomenology of aggregation, we have switched off the attraction between dimers and spheres. In this case, even though an (effective depletion) attraction between spheres is present, the global picture of the mixture is that of a homogeneous fluid. Hence, for at least the modelization and thermodynamic conditions investigated in this work, depletion forces alone are not sufficient to induce cluster formation or phase separation in our mixture.

The present results provide more insight into the complex behaviour of colloidal mixtures, including the interplay between explicit attractive interactions and depletion forces.

Acknowledgements

This work has been done using the computer facilities made available by the PO-FESR 2007-2013 Project MedNETNA (Mediterranean Network for Emerging Nanomaterials).

References

[1] W.B. Russel, D.A. Saville, W.R. Schowalter, Colloidal Dispersions, Cambridge University Press, 1991.
[2] Y.D. Yin, Y. Lu, B. Gates, Y.N. Xia, Template-assisted self-assembly: a practical route to complex aggregates of monodispersed colloids with well-defined sizes, shapes, and structures, J. Am. Chem. Soc. 123 (2001) 8718.
[3] S.C. Glotzer, M.J. Solomon, N.A. Kotov, Self-assembly: from nanoscale to microscale colloids, AIChE J. 50 (12) (2004) 2978.
[4] G. Yi, V.N. Manoharan, E. Michel, M.T. Elsesser, S. Yang, D.J. Pine, Colloidal clusters of silica or polymer microspheres, Adv. Mater. 16 (14) (2004) 1204–1207.
[5] D. Zerrouki, J. Baudry, D. Pine, P. Chaikin, J. Bibette, Chiral colloidal clusters, Nature 455 (2008) 381.
[6] Q. Chen, S.C. Bae, S. Granick, Directed self-assembly of a colloidal kagome lattice, Nature 469 (2011) 381.
[7] S. Sacanna, D.J. Pine, Shape-anisotropic colloids: building blocks for complex assemblies, Curr. Opin. Colloid Interface Sci. 16 (2011) 96.
[8] X. Mao, Q. Chen, S. Granick, Entropy favours open colloidal lattices, Nat. Mat. 12 (2013) 217.
[9] A. Yethiraj, A. van Blaaderen, A colloidal model system with an interaction tunable from hard sphere to soft and dipolar, Nature 421 (2003) 513–517.
[10] Y. Wang, Y. Wang, D.R. Breed, V.N. Manoharan, L. Feng, A.D. Hollingsworth, M. Weck, D. Pine, Colloids with valence and specific directional bonding, Nature 491 (2012) 51.
[11] R. McGorty, J. Fung, V.N. Manoharan, Colloidal self-assembly at an interface, Mater. Today 13 (2010) 34.
[12] M. Chen, H. Li, A.F. Mejia, X. Wang, Z. Cheng, Observation of isotropic–isotropic demixing in colloidal platelet-sphere mixtures, Soft Matter 11 (2015) 5775.
[13] M. Adams, Z. Dogic, S.L. Keller, S. Fraden, Entropically driven microphase transitions in mixtures of colloidal rods and spheres, Nature 393 (1998) 349.
[14] D.A. Christian, A. Tian, W.E. Ellenbroek, I. Levental, K. Rajagopal, P.A. Janmey, A.J. Liu, T. Baumgart, D.E. Discher, Spotted vesicles, striped micelles and Janus assemblies induced by ligand binding, Nat. Mater. 8 (2009) 843.
[15] J.P. Hansen, I.R. McDonald, Theory of Simple Liquids with Applications to Soft Matter, 4th ed., Academic Press, New York, 2013.
[16] F. Sciortino, S. Mossa, E. Zaccarelli, P. Tartaglia, Equilibrium cluster phases and low-density arrested disordered states: the role of short-range attraction and long-range repulsion, Phys. Rev. Lett. 93 (5) (2004) 055701.
[17] E. Zaccarelli, Colloidal gels: equilibrium and non-equilibrium routes, J. Phys.: Condens. Matter 19 (2007) 323101.
[18] P.J. Lu, E. Zaccarelli, F. Ciulla, A.B. Schofield, F. Sciortino, D.A. Weitz, Gelation of particles with short-range attraction, Nature 453 (2008) 499–503.
[19] N.B. Wilding, F. Schmid, P. Nielaba, Liquid–vapor phase behavior of a symmetrical binary fluid mixture, Phys. Rev. E 58 (1998) 2201.
[20] A. Goyal, C.K. Hall, O.D. Velev, Self-assembly in binary mixtures of dipolar colloids: molecular dynamics simulations, J. Chem. Phys. 133 (2010) 064511.
[21] C.N. Likos, Effective interactions in soft condensed matter physics, Phys. Rep. 348 (2001) 267.
[22] A.A. Louis, E. Allahyarov, H. Lowen, R. Roth, Effective forces in colloidal mixtures: from depletion attraction to accumulation repulsion, Phys. Rev. E 65 (2002) 061407.
[23] N. Gnan, E. Zaccarelli, P. Tartaglia, F. Sciortino, How properties of interacting depletant particle control aggregation of hard-sphere colloids, Soft Matter 8 (2012) 1991.
[24] A. Parola, L. Reatto, Depletion interaction between spheres of unequal size and demixing in binary mixtures of colloids, Mol. Phys. 113 (2015) 2571.
[25] M. Kamp, M. Hermes, C.M. van Kats, D.J. Kraft, W. Kegel, M. Dijkstra, A. van Blaaderen, Selective depletion interactions in mixtures of rough and smooth silica spheres, Langmuir 32 (2016) 1233.
[26] M. Dijkstra, R. van Roij, R. Evans, Phase behavior and structure of binary hard-sphere mixtures, Phys. Rev. Lett. 81 (1998) 2268.
[27] M. Dijkstra, R. van Roij, R. Evans, Phase diagram of highly asymmetric binary hard-sphere mixtures, Phys. Rev. E 59 (1999) 5744.
[28] S. Whitelam, S.A.F. Bon, Self-assembly of amphiphilic peanut-shaped nanoparticles, J. Chem. Phys. 132 (2010) 074901.
[29] T.S. Skelhon, Y. Chen, S.A.F. Bon, Synthesis of "hard–soft" Janus particles by seeded dispersion polymerization, Langmuir 30 (2014) 13525.
[30] L. Feng, R. Dreyfus, R. Sha, N.C. Seeman, P.M. Chaikin, DNA patchy particles, Adv. Mater. 25 (2013) 2779.
[31] E. Slyk, W. Rzysko, P. Bryk, Two-dimensional binary mixtures of patchy particles and spherical colloids, Soft Matter 12 (2016) 9538.
[32] J.R. Wolters, J.E. Verweij, G. Avvisati, M. Dijkstra, W.K. Kegel, Depletion induced encapsulation by dumbbell-shaped patchy colloids stabilize microspheres against aggregation, Langmuir 33 (2017) 2370.
[33] S. Prestipino, G. Munaò, D. Costa, C. Caccamo, Self-assembly in a model colloidal mixture of dimers and spherical particles, J. Chem. Phys. 146 (2017) 084902.
[34] G. Munaò, D. Costa, S. Prestipino, C. Caccamo, Encapsulation of spherical nanoparticles by colloidal dimers, Phys. Chem. Chem. Phys. 18 (2016) 24922.
[35] R.A.L. Jones, Soft Condensed Matter, Oxford University Press, 2002.
[36] J. Hoshen, R. Kopelman, Percolation and cluster distribution. I. Cluster multiple labeling technique and critical concentration algorithm, Phys. Rev. B 14 (1976) 3438.
[37] D. Stauffer, Scaling theory of percolation clusters, Phys. Rep. 54 (1979) 1.
[38] S.-H. Chen, J. Rouch, F. Sciortino, P. Tartaglia, Static and dynamic properties of water-in-oil microemulsions neat the critical and percolation points, J. Phys.: Condens. Matter 6 (1994) 10855.
[39] P.D. Godfrin, R. Castañeda-Priego, Y. Liu, N.J. Wagner, Intermediate range order and structure in colloidal dispersions with competing interactions, J. Chem. Phys. 139 (2013) 154904.
[40] P.D. Godfrin, N.E. Valadez-Pérez, N.J. Wagner, Y. Liu, Generalized phase behavior of cluster formation in colloidal dispersions with competing interactions, Soft Matter 10 (2014) 5061.
[41] L. Bai, D. Breen, Calculating center of mass in an unbounded 2D environment, J. Gr. GPU Game Tools 13 (2008) 53.
[42] https://en.wikipedia.org/wiki/Center_of_mass.